The Astrophysical Journal, 575:137–144, 2002 August 10

SPECTRAL ENERGY DISTRIBUTIONS OF FLAT-SPECTRUM RADIO QUASARS OBSERVED WITH *BeppoSAX*

F. Tavecchio,[1] L. Maraschi,[1] G. Ghisellini,[2] A. Celotti,[3] L. Chiappetti,[4] A. Comastri,[5] G. Fossati,[6] P. Grandi,[7] E. Pian,[8] G. Tagliaferri,[2] A. Treves,[9] and R. Sambruna[10]

Received 2001 December 18; accepted 2002 April 15

ABSTRACT

We report the *BeppoSAX* observations of six flat-spectrum radio quasars. Three of them have a clear detection up to 100 keV with the PDS instrument. For four objects the X-ray spectrum is satisfactorily fitted by a power-law continuum with Galactic absorption. QSO 2251+158 shows the presence of absorption higher than the Galactic value, while the spectrum of the source QSO 0208−512 shows a complex structure, with evidence of absorption at low energy. We construct the spectral energy distributions adding historical data to the broadband X-ray spectra obtained with *BeppoSAX* and reproduce them with a one-zone synchrotron–inverse Compton model (including both synchrotron self-Compton and external Compton). The implications are briefly discussed.

Subject headings: quasars: general — quasars: individual (QSO 0208−512, QSO 0521−365, QSO 1641+399, QSO 2223−052, QSO 2243−123, QSO 2251+158) — radiation mechanisms: nonthermal — X-rays: galaxies

1. INTRODUCTION

Blazars are the best laboratory for studying the physics of relativistic jets. The nonthermal continuum amplified by relativistic beaming (e.g., Urry & Padovani 1995) is a unique tool to probe the physical processes acting in the jet. In the last decade the interest in blazars has been renewed by the EGRET discovery of 66 blazars (Hartman et al. 1999) as strong γ-ray emitters. In several cases the γ-ray emission dominates the apparent bolometric luminosity. Moreover, the short variability timescales, together with the absence of absorption of high-energy photons (through the $\gamma\gamma$ pair production), directly imply that the γ-ray emission is also relativistically beamed (e.g., Dondi & Ghisellini 1995).

Despite the large variety of classifications, there is growing evidence that blazars form a single population. Their different spectral properties can be unified within a spectral sequence in which the leading parameter is the total luminosity (Fossati et al. 1998). At the high-luminosity extreme of the sequence we find the flat-spectrum radio quasars (FSRQs), the most luminous blazars, characterized by the presence of bright emission lines in the optical–UV spectrum and, in some cases, strong *UV bumps*, signatures of the underlying accretion process (e.g., Pian et al. 1999 and references therein). Most of the blazars detected by EGRET (Hartman et al. 1999) belong to this subclass, but not all FSRQs with comparable spectral energy distributions (SEDs) have been detected in the γ-ray domain.

In the study of FSRQs, observations in the X-ray band play a fundamental role. The X-ray emission from an FSRQ is dominated by the continuum originating from inverse Compton scattering between relativistic electrons in the jet and the soft photons produced by the disk and/or in the broad-line region (BLR; Dermer & Schlickeiser 1993; Sikora, Begelman, & Rees 1994). The possibility of measuring the inverse Compton (IC) component yields important constraints on the emission models. Moreover, the study of the soft X-ray spectrum (below 1 keV) provides insight on the presence of intrinsic absorption, on the possible contribution of the high-energy end of the synchrotron emission, or on the minimum energy of emitting particles. The latter point is particularly interesting because the determination of the minimum energy of particles is a fundamental step in the estimate of the total power transported by the jet (e.g., Celotti, Padovani, & Ghisellini 1997).

The *BeppoSAX* satellite has the unique capability of covering the wide energy range 0.1–200 keV. For this reason it is ideal for studying FSRQs. In particular, the knowledge of the spectrum in this band, together with the γ-ray spectrum measured by EGRET, provide the most complete spectral information on the high-energy component (see, e.g., Tavecchio et al. 2000, hereafter Paper I). For these reasons we started an observational program with *BeppoSAX* of a sample of FSRQs (containing a total of 50 sources) extracted from the 2 Jy sample by Padovani & Urry (1992). Using the flux threshold $F_{1\,\mathrm{keV}} > 0.5$ μJy reduces the number of sources to 19. In Paper I we discussed the case of three FSRQs detected by EGRET, namely, QSO 0836+710, QSO 1510−089, and QSO 2230+114. Here we report the analysis of *BeppoSAX* data of six other sources, three detected by EGRET and three without an EGRET detection. With the

[1] Osservatorio Astronomico di Brera, via Brera 28, 20121 Milan, Italy.
[2] Osservatorio Astronomico di Brera, via Bianchi 46, 23807 Merate, Italy.
[3] SISSA/International School for Advanced Studies, via Beirut 2-4, 34014 Trieste, Italy.
[4] IFC/CNR, via Bassini 15, 20133 Milan, Italy.
[5] Osservatorio Astronomico di Bologna, via Ranzani 1, 40127 Bologna, Italy.
[6] Center for Astrophysics and Space Sciences, University of California, San Diego, CA 92093-0424.
[7] IAS, IAS/CNR, via Fosso del Cavaliere, 00133 Rome, Italy.
[8] Osservatorio Astronomico di Trieste, via Tiepolo 11, 24131 Trieste, Italy.
[9] Università dell'Insubria, via Valleggio 11, 22100 Como, Italy.
[10] George Mason University, 4400 University Drive, M/S 3F3, Fairfax, VA 22030-4444.

TABLE 1
LIST OF THE SOURCES DISCUSSED IN THE PRESENT WORK

Source	Other Name	z	EGRET
0208−512.....	PKS	1.003	Yes
0521−365.....	PKS	0.055	Yes
1641+399.....	3C 345	0.593	No
2223−052.....	3C 446	1.4	No
2243−123.....	PKS	0.63	No
2251+158.....	3C 454.4	0.859	Yes

NOTE.—The last column indicates EGRET detection or lack thereof.

addition of these six sources to the three FSRQs analyzed in Paper I and three other sources (3C 279, QSO 0528+134, PKS 0537−441) discussed elsewhere (Maraschi et al. 1998; Ghisellini et al. 1999; Pian et al. 2002), a total of 12 FSRQs (of 19 with X-ray flux $F_{1\,\mathrm{keV}} > 0.5$ μJy) from the 2 Jy sample were observed by *BeppoSAX*. The sources discussed here are listed in Table 1. Partial and preliminary results were reported in Maraschi & Tavecchio (2001).

The paper is organized as follows: in § 2 we report the analysis of *BeppoSAX* observations, in § 3 we discuss the emission models for the SEDs, and finally in § 4 we discuss our results.

2. *BeppoSAX* OBSERVATIONS AND ANALYSIS

The scientific payload of the *BeppoSAX* satellite (see Boella et al. 1997) contains four co-aligned narrow-field instruments (NFIs) and two wide-field cameras. Two of the NFIs use concentrators to focalize X-rays: the low-energy concentrator spectrometer (LECS) has a detector sensitive to soft–medium X-ray photons (0.1–10 keV), while the medium concentrator spectrometer (MECS) can detect photons in the medium-energy range 1.3–10 keV. The phoswich detector system (PDS), sensitive from 12 up to 200 keV, consisting of four identical units, uses rocking collimators so as to monitor source and background simultaneously with interchangeable units. We will not be concerned here with the fourth NFI, a high-pressure gas scintillation proportional counter.

The *BeppoSAX* journal of observations is reported in Table 2, with exposure times and observed count rates. None of the sources showed significant flux variations during the observations. We therefore obtained a cumulative spectrum for each source.

We analyzed the *BeppoSAX* spectral data using the standard software packages XSELECT (Version 1.4b) and XSPEC (Version 11.0) and the 1997 September version of the calibration files released by the *BeppoSAX* Scientific Data Center (SDC). From the event files we extracted the LECS and MECS spectra in circular regions centered around the source with radii of 8′ and 4′, respectively (see the *SAX* Analysis Cookbook[11]). The PDS spectra extracted with the standard pipeline with the rise-time correction were directly provided by the *BeppoSAX* SDC. We used PDS data rebinned with signal-to-noise ratio greater than 3.

For the spectral analysis we considered the LECS data in the restricted energy range 0.1–4 keV, because of known unsolved problems with the response matrix at higher energies. Background spectra extracted from blank-field observations at the same position as the source were used. We fitted rebinned LECS, MECS, and PDS spectra jointly, allowing for two variable different normalization factors to take into account uncertainties in the intercalibration of different instruments (see *SAX* Cookbook).

The first model chosen for the fitting procedure was in all cases a single power law plus Galactic absorption. In the following we discuss in detail the results for each source. The results of the spectral fits are summarized in Tables 3 and 4.

2.1. *QSO 0208−512*

The residuals of a simple power-law model fit to the LECS + MECS data show the presence of a prominent absorption feature, located at ∼0.6 keV (see Fig. 1), and an excess at about 5 keV. Inspection of the individual MECS2 and MECS3 spectra reveals that the emission feature at 5 keV is present only in the data obtained with the MECS3, indicating an instrumental origin. Only the MECS2 data are used below.

The low-energy feature can be modeled either with an absorption edge ($E = 0.60^{0.75}_{0.33}$; see Fig. 2) or with an absorption trough ($E = 0.89^{0.94}_{0.80}$) with comparable probability ($\chi^2_r = 0.72$ [$P = 0.72$] and $\chi^2_r = 0.78$ [$P = 0.75$], respectively). However, these features find no obvious interpretation at the redshift of the source. We then tried a warm absorber model (ABSORI of XSPEC), at the redshift of the quasar, obtaining a satisfactory fit ($\chi^2_r = 0.89$). The fit requires a column density of the absorber equal to $N_{\mathrm{H}} = 1.2^{10.3}_{1.2} \times 10^{22}$ cm^{-2} and an ionization parameter

[11] See http://www.asdc.asi.it/bepposax/software/index.html.

TABLE 2
BeppoSAX DATA OBSERVATION LOG

Source	Date	Start	End	LECS Exposure (s)	Net counts s^{-1}[a]	MECS Exposure (s)	Net counts s^{-1}[b]	PDS Exposure (s)	Net counts s^{-1}
0208−512.....	2001 Jan 14–15	13:37:10	13:00:09	15,650	0.022 ± 0.001	34,256	0.053 ± 0.001	15,260	0.1417 ± 0.03
0521−365.....	1998 Oct 2–3	10:16:24	09:46:23	17,752	0.067 ± 0.002	41,082	0.106 ± 0.001	19,052	0.05 ± 0.04
1641+399.....	1999 Feb 19	03:55:43	20:13:57	10,934	0.045 ± 0.002	25,866	0.059 ± 0.002	13,052	0.15 ± 0.05
2223−052.....	1997 Nov 10–11	13:22:27	00:22:40	9200	0.01 ± 0.001	16,180	0.016 ± 0.001	6860	0.008 ± 0.08
2243−123.....	1998 Nov 18–19	18:41:31	11:49:58	10,060	0.015 ± 0.002	27,500	0.022 ± 0.001	13,222	0.004 ± 0.015
2251+158.....	2000 Jun 5–6	15:36:05	21:44:38	17,425	0.046 ± 0.001	48,515	0.115 ± 0.002	22,439	0.29 ± 0.03

[a] 0.1–4 keV.
[b] 1.8–10.5 keV, 2 MECS units.

TABLE 3
ABSORBED POWER-LAW FITS TO *BeppoSAX* DATA

Source	Γ^a	N_H ($\times 10^{20}$ cm^{-2})	$F_{2-10\,keV}$ ($\times 10^{-12}$ ergs cm^{-2} s^{-1})	χ^2/dof
0208−512 (LE + ME2+PDS)[b]	$1.68^{1.80}_{1.51}$	$16.7^{30.0}_{0.1}$	4.7	51.16/28
0521−365 (LE + ME)	$1.77^{1.85}_{1.73}$	$4.3^{7.6}_{3.2}$	8.72	69.35/89
1641+399 (LE + ME+PDS)	$1.57^{1.66}_{1.47}$	1.12 (fix)	5.2	65.26/45
2223−052 (LE + ME)	$1.84^{2.27}_{1.56}$	$7.1^{76.1}_{0}$	1.25	14./16
	$1.86^{2.15}_{1.58}$	4.87 (fix)	...	14.72/17
2243−123 (LE + ME)	$1.73^{1.91}_{1.56}$	$3.05^{7.7}_{1.28}$	1.83	18.37/23
2251+158 (LE + ME+PDS)	$1.31^{1.26}_{1.36}$	6.5 (fix)	10.6	94.2/80
	$1.38^{1.33}_{1.44}$	$18.6^{25.1}_{12.2}$	...	77.1/79

NOTE.—Errors are quoted at the 90% confidence level for one parameter of interest.
[a] Photon index, related to the spectral index by $\alpha = \Gamma + 1$.
[b] See Table 4.

$\xi = 262^{853}_{32}$, providing a reasonable physical interpretation. The results of the fits are reported in Table 4.

Previous *ROSAT* (Sambruna 1997) and *ASCA* (Kubo et al. 1998) spectra show a power-law X-ray spectrum with photon index $\Gamma_{2-10\,keV} = 1.7 \pm 0.1$, similar to that found with *BeppoSAX*. Notably, these observations (with comparable flux) showed a smooth continuum, without any evidence for spectral features.

The PDS/MECS normalization factor required by the data (2.7 ± 1.3) is well above the 90% upper limit (0.93) given by the *SAX* Cookbook. QSO 0208−512 is located in a rich field: although the LECS and MECS images do not show other sources, a search using the NASA Extragalactic Database[12] reveals the presence of 13 sources cataloged as QSOs or X-ray sources, within a circular region with radius 1° centered on our target. It is then possible that the high-energy spectrum is contaminated by one or more sources present in the field of view (~1°) of the PDS.

In the fit presented here the PDS data are not included.

2.2. *QSO 0521−365*

The LECS+MECS spectrum is well fitted by an absorbed power law ($\Gamma = 1.77$ [1.73–1.85]) with column density consistent with the Galactic value. Previous X-ray observations with *EXOSAT* ($\Gamma \sim 1.6$; Pian et al. 1996) and *ROSAT* ($\Gamma = 1.92 \pm 0.05$; Sambruna 1997) are consistent with our results.

[12] See http://nedwww.ipac.caltech.edu/index.html.

TABLE 4
FITS TO *BeppoSAX* DATA OF 0208−512

Model	Γ^a	E_{abs} or $N_H{}^b$	τ or ξ^c	χ^2/dof
PL + edge	$1.72^{1.88}_{1.65}$	$0.56^{0.75}_{0.33}$	$2.1^{10}_{0.9}$	13.25/17
PL + notch	$1.68^{1.81}_{1.55}$	$0.89^{0.94}_{0.80}$	$0.21^{0.31}_{0.13}$	12.85/17
PL + ABSORI	$1.70^{1.96}_{1.62}$	$4.2^{10.3}_{1.2}$	262^{853}_{32}	15.13/17

NOTE.—Errors are quoted at the 90% confidence level for one parameter of interest.
[a] Photon index, related to the spectral index by $\alpha = \Gamma + 1$.
[b] Energy of the absorption feature (keV) or N_H for ABSORI (in units of 10^{20} cm^{-2}).
[c] Optical depth for the edge, width (keV) for NOTCH or ξ for ABSORI.

2.3. *QSO 1641+399 (3C 345)*

A power-law model ($\Gamma \simeq 1.6$) with Galactic absorption fits the MECS + PDS data for $E > 2$ keV up to ~200 keV.

The inspection of the LECS image reveals the presence of several sources (not present in the MECS image): in particular a low-luminosity Seyfert galaxy, NGC 6212, located 5′ away from the quasar hence within the standard extraction region of the LECS data. We conclude that the LECS spectrum could be contaminated by the presence of other sources close to 1641+399. In fact, the residuals of a fit with an absorbed power-law model of the LECS data alone ($\Gamma \simeq 1.8$, $\chi^2_r = 2.7$) show large scatter around the model (Fig. 3), with the presence of possible features (with no

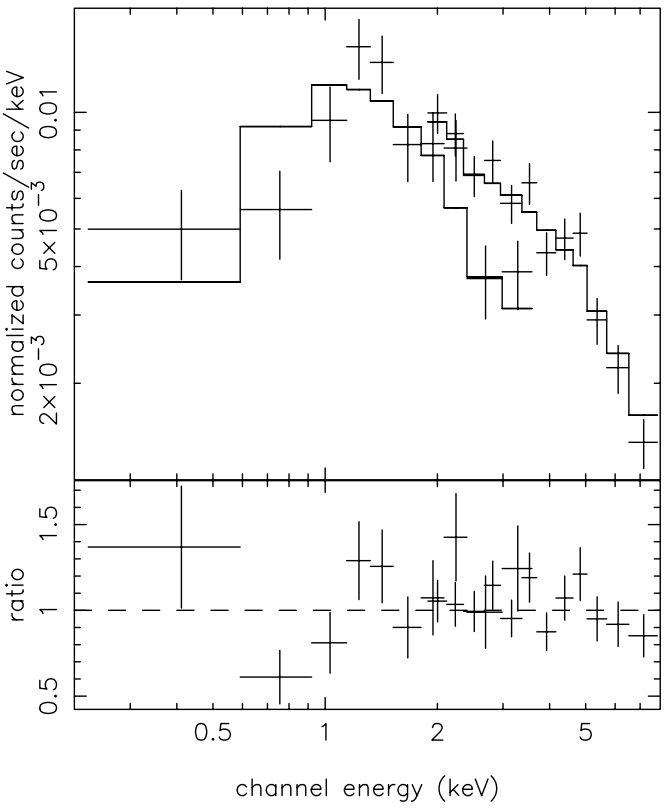

FIG. 1.—Fit of LECS and MECS data of 0208−512 with a power law and free absorption. The feature at ~0.6 keV is clearly visible in the data-to-model ratio (*lower panel*).

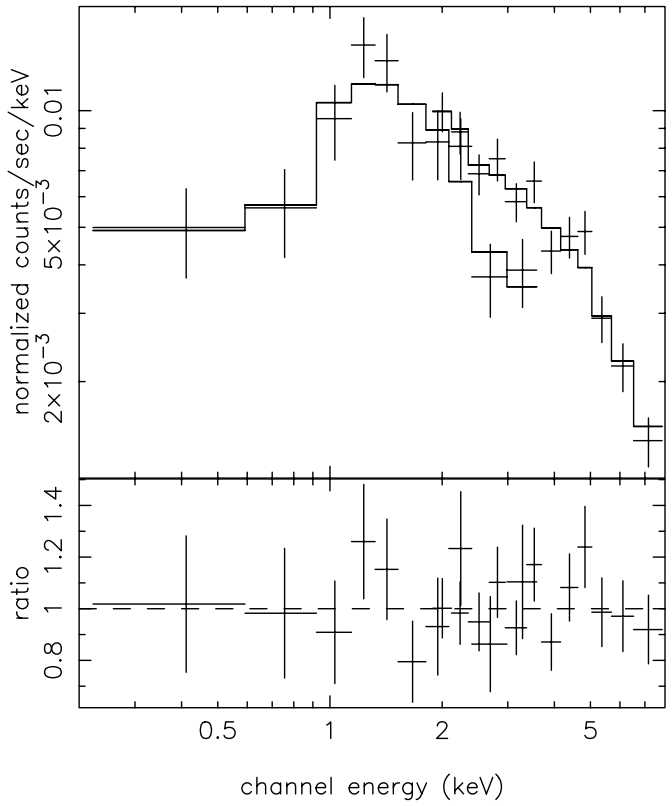

FIG. 2.—Fit of LECS and MECS data of 0208−512 with a power law (Galactic absorption) plus an absorption edge.

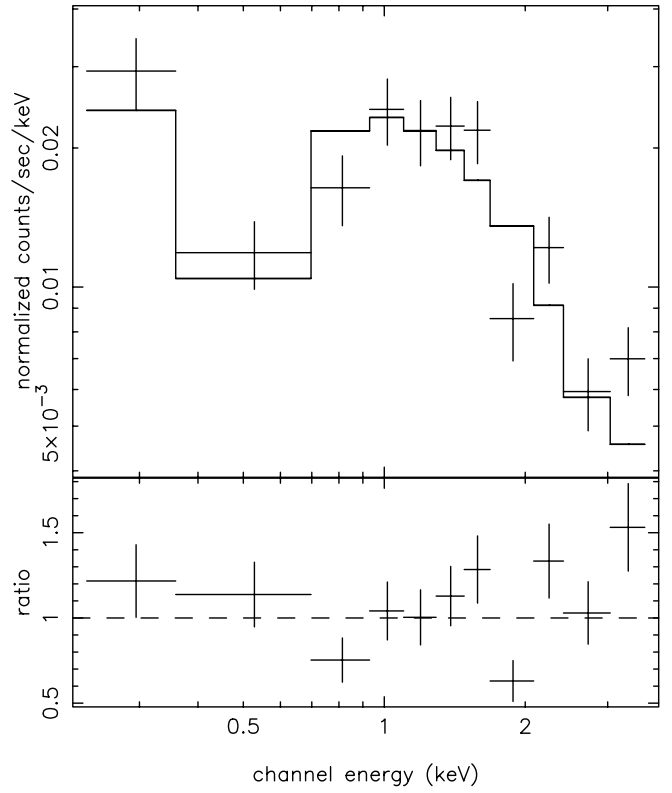

FIG. 3.—Fit of LECS data of 1641+399 with a power law and Galactic absorption.

straightforward interpretation) at energies of ∼2 keV and below ∼1.0 keV. The features cannot simply be modeled as due to absorption of the continuum by a warm absorber at the redshift of the source.

A clear soft excess, interpreted as the hard tail of the UV bump, was present in the *ROSAT* data discussed by Sambruna (1997).

2.4. *QSO 2223−052 (3C 446)*

An absorbed power law with Galactic absorption provides a good fit to the data. Our spectrum ($\Gamma \simeq 1.85$) is steeper than that measured on one occasion by *Ginga* ($\Gamma = 1.3$; Lawson & Turner 1997). Moreover, we do not confirm the *ROSAT* observations that seem to indicate an absorption column higher than the Galactic value at the 99% confidence level (Sambruna 1997).

2.5. *QSO 2243−123*

A power law with intermediate spectral index ($\Gamma = 1.7$) fits the data well.

The *ROSAT* observation reported by Siebert et al. (1998) showed a very steep spectrum, with $\Gamma = 2.9 \pm 0.5$ and a flux about 2.5 times larger than during our *BeppoSAX* pointing. Given the large flux variation, the steep spectrum measured by *ROSAT* could possibly represent intrinsic spectral variability possibly due to the high-energy end of the synchrotron component, extending up to the soft X-ray band.

2.6. *QSO 2251+158 (3C 454.4)*

As shown in Table 3, a fit with a power-law model and Galactic absorption gives an unacceptable fit to the data. When we use a free value for $N_{\rm H}$, the fit improves significantly, requiring a column density higher than the Galactic value at the 99% confidence level (see the contour plot in Fig. 4). The value of the required absorption column density in the quasar rest frame is $N_{\rm H,\,int} = 4.9^{7.9}_{2.4} \times 10^{21}$ cm^{-2}.

An acceptable fit ($\chi_r = 0.93$) of the low-energy portion of the spectrum can also be obtained with a broken power-law model (and Galactic column density), with a very flat ($\Gamma = -0.25$) soft spectrum. This, as in the case of other sources (e.g., 0836−710; Paper I), could be due to an intrinsic break in the continuum. From a statistical point of view both models have almost the same probability.

3. MODELING THE SEDS

Using *BeppoSAX* and historical data, we assembled the SEDs of the sources, shown in Figure 5. EGRET data are the average over the available observations as given by Hartman et al. (1999), while upper limits are from Thompson et al. (1995). For 0208−512 we report also the COMPTEL detection reported in Blom et al. (1995).

In the IR–optical bands, for 2223−052 are available quasi-simultaneous *Infrared Space Observatory* (reported in Haas et al. 1998) and optical data. For three other sources (1641+399, 2243−123, 2251+158) we report average optical fluxes with the observed variability range. For 1641+399 Xie et al. (1999) report a variability amplitude in the *B* band $\Delta B \simeq 3$ mag (which is shown in Fig. 5), while for the other two sources the variability observed is rather small (less than 1 mag). For 0208−512 and 0521−365 we report only the data we could find in the literature. Both sources have

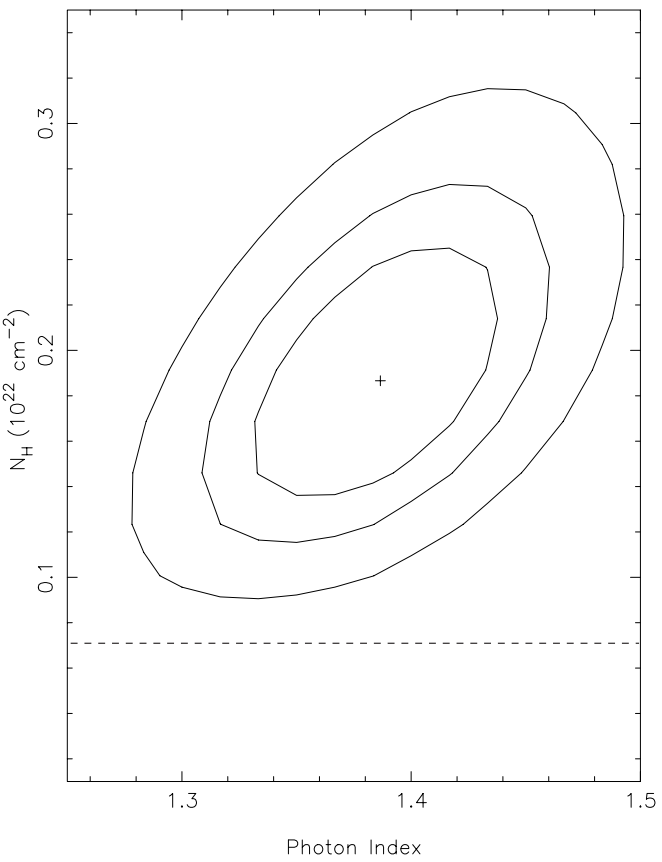

FIG. 4.—68%, 90%, and 99% photon index–N_H confidence contours for 2251+158. The column density exceeds the Galactic value at a greater than 99% level.

IUE data. References to the data are reported in the figure legend.

The double-humped shape of the SEDs is widely interpreted as due to synchrotron-IC emission. The low-energy component is synchrotron radiation from a population of relativistic electrons, while the high-energy component is believed to be produced through IC scattering of soft photons by the same electrons (although other scenarios have been considered, e.g., hadronic models; see Mannheim & Biermann 1992). The nature of soft photons involved in the IC process is still debated. In blazars where thermal features (emission lines, the *blue bump*) are weak or even absent (as in BL Lac objects) the energy density of target photons is probably dominated by those produced by synchrotron (synchrotron self-Compton [SSC] model; e.g., Maraschi, Ghisellini, & Celotti 1992), while in powerful quasars (FSRQs) photons coming into the jet from the external environment form the dominant population (external Compton [EC] model; Dermer & Schlickeiser 1993; Sikora et al. 1994).

We have reproduced the overall SEDs using a Synchrotron–inverse Compton (SSC+EC) model. The source is modeled as a sphere with radius R, tangled magnetic field with intensity B, in motion with bulk Lorentz factor Γ_b at an angle θ with respect to the line of sight. Relativistic effects are then regulated by the relativistic Doppler factor, given by $\delta = [\Gamma_b(1 - \beta\cos\theta)]^{-1}$. Usually, for blazars $\theta \sim 1/\Gamma_b$, implying $\delta \simeq \Gamma_b$. Relativistic electrons emit through synchrotron and IC mechanisms. IC emissivity is calculated taking into account the full Klein-Nishina cross section (following the Jones 1968 treatment). The electron energy distribution is modeled with the form

$$N(\gamma) = K\gamma^{-n_1}\left(1 + \frac{\gamma}{\gamma_b}\right)^{n_1 - n_2}, \quad (1)$$

where K is a normalization factor, γ_b is the break Lorentz factor, and n_1 and n_2 are the spectral indices below and above the break, respectively. This particular form for the distribution function has been assumed on a purely phenomenological basis, in order to describe the curved shape of the SED.

The external radiation field is modeled as a blackbody peaking at $\nu_{\rm ext} \simeq 10^{15}$ Hz and energy density $U_{\rm ext}$. The last quantity is calculated assuming that the radiation, with total luminosity $\tau L_{\rm ext}$ (τ, usually assumed to be $\sim$0.1, is the fraction of the central emission reprocessed by the BLR), is diluted into a sphere of radius $R_{\rm BLR}$. For 2251+158, which shows a clear UV bump, we take $L_{\rm ext} = L_{\rm UV}$, while for the other cases we inferred $L_{\rm ext}$ from the luminosity of broad emission lines, following the approach used by Celotti et al. (1997). Luminosities are reported in Table 5. The value of $R_{\rm BLR}$ has been chosen to fit the observed data, but we checked that it is close to the value expected from the relation between the luminosity of the BLR and the radius derived (for radio-quiet quasars) by Kaspi et al. (2000). The external radiation energy density is amplified in the blob's rest frame by a factor of Γ^2 (e.g., Ghisellini et al. 1998). Moreover, as pointed out by Dermer et al. (1995; and confirmed by Georganopoulos, Kirk, & Mastichiadis 2001), because of relativistic effects, the beaming pattern of the EC radiation is narrower than that of the SSC emission. However, when $\delta \simeq \Gamma$ (as assumed here), the amplification is the same for both processes.

With these assumptions the model is well constrained by the observation and we can obtain fairly robust estimates of the principal physical quantities in the jet (see Paper I). The values of the parameters used to reproduce the SEDs are reported in Table 5. In all cases the bulk of the IC component is reproduced with the EC emission, while in some cases the SSC spectrum (peaking at lower energies) partly accounts for the low-energy portion of the X-ray spectrum. The cutoff in the synchrotron spectrum around 10^{11} Hz is due to self-absorption. Clearly, the adopted one-zone model cannot account for the radio emission, widely considered to be due to the superposition of the emission produced in the outer ($d \gtrsim 0.1$ pc) regions of the jet (e.g., Blandford & Königl 1979).

4. DISCUSSION AND CONCLUSIONS

We have presented the results of the analysis of six FSRQs observed with *BeppoSAX*. The smooth power-law ($\Gamma = 1.6$–1.7) X-ray continuum is produced through IC scattering on photons external to the jet, except for the "atypical" source 0521−365. In the case of two sources, 0208−512 and 2251+158, there is evidence of more complex X-ray spectra. In particular, 0208−512 shows an absorption feature at $\sim$0.6 keV, that we suggest could be explained allowing the presence of a warm absorption intercepting the emission produced in the jet.

The soft X-ray spectrum of 2251+158 shows a clear deficit of photons, consistent with either an intrinsic absorption

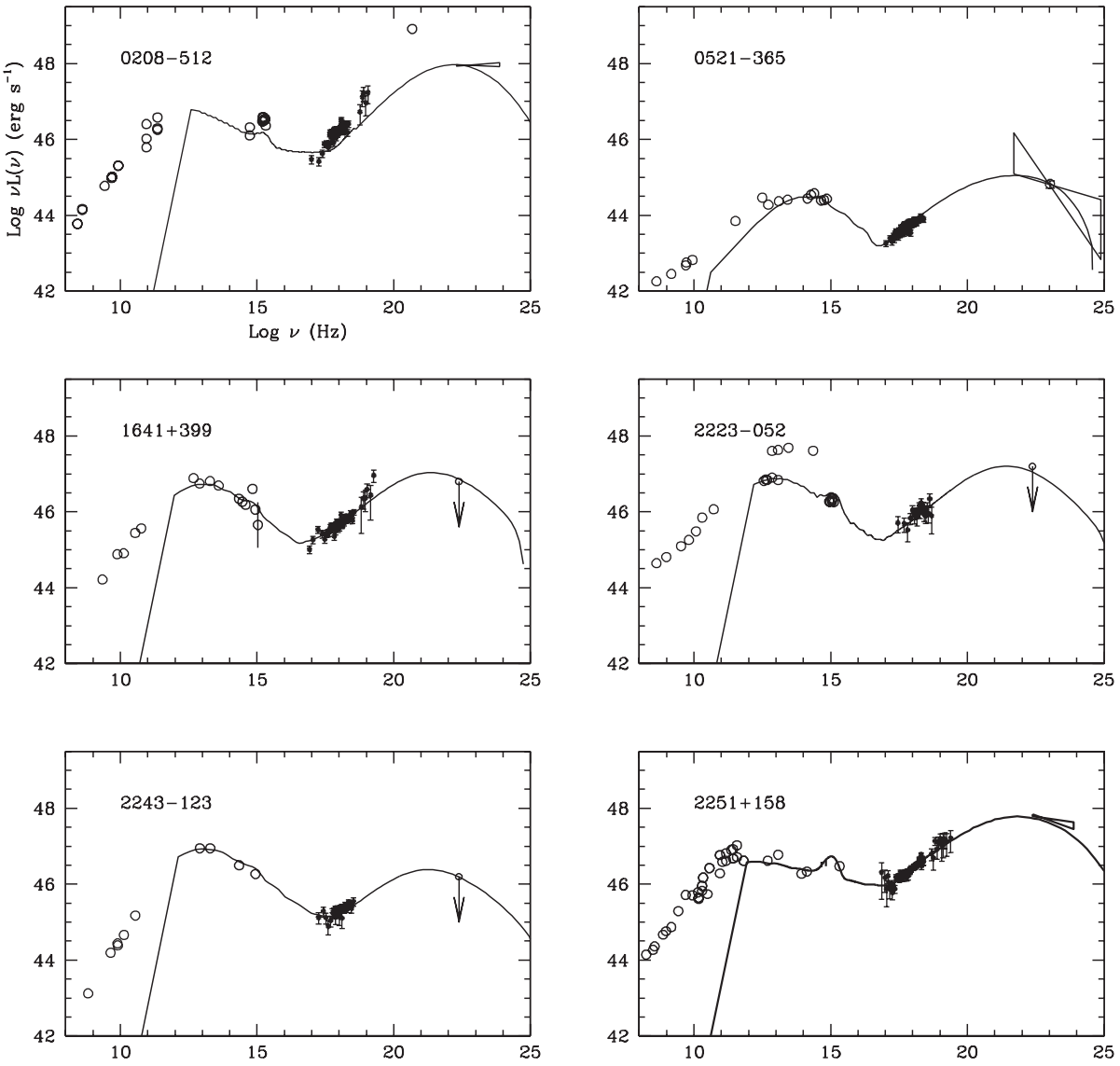

FIG. 5.—SEDs of the sources analyzed in this work. The solid line is the model discussed in the text. References for the data: 0208−512: Bertsch et al. (1993); Tornikoski et al. (1996); Stacy et al. (1996); Impey & Tapia (1988); Blom et al. (1995). 0521−365: Wright & Otrupcek (1990); Wright et al. (1996); Glass et al. (1981); Falomo et al. (1993); Xie et al. (1998). 1641+339: Wiren et al. (1992); Patnaik et al. (1992); Geogory & Condon (1991); Moshir et al. (1990); Neugebauer et al. (1982); Villata et al. (1997); Xie et al. (1998). 2223−052: Wright & Otrupcek (1990); Haas et al. (1998); OPTICAL. 2243−123: Wright & Otrupcek (1990); Wright, Ables, & Allen (1983); Kotilainen, Falomo, & Scarpa (1998); Garcia et al. (1999). 2251+158: Kühr et al. (1981); NED; Gear et al. (1994); Stevens et al. (1994); Impey & Neugebauer (1988); Smith et al. (1988); Pian & Treves (1993).

TABLE 5

PARAMETERS USED FOR THE EMISSION MODEL DESCRIBED IN THE TEXT

Source	R ($\times 10^{16}$ cm)	B (G)	δ	γ_b	n_1	n_2	K (cm^{-3})	$L_{\rm BLR}$ ($\times 10^{45}$ ergs s^{-1})	$R_{\rm BLR}$ ($\times 10^{18}$ cm)
0208−512.....	1.5	1.5	18	100	1.4	3.8	2×10^4	2.1	0.6
0521−365.....	2.0	0.3	3[a]	8.8×10^3	1.25	4	3×10^3	2.4×10^{-2}	0.8
1641+399.....	4.0	2.9	9.75	200	1.5	4.2	2.8×10^3	3.7	0.6
2223−052.....	4.25	5.6	17	135	1.6	4.3	1.7×10^3	8.5	1.1
2243−123.....	3.5	2.5	15	250	1.6	4.3	1.7×10^3	5.6	0.9
2251+158.....	4.0	1.5	12	60	1.8	3.4	5×10^4	4.	1.0

[a] See text.

(with rest-frame column density $\sim 5 \times 10^{21}$ cm^{-2}) or an intrinsic break in the continuum occurring below $\sim$1 keV. In the latter case the position of the break could provide important insights into the physics of the jet, in particular regarding the value of the minimum energy of the radiating particles. On the other hand, there is growing evidence that the presence of intrinsic absorption is common in high-redshift radio-loud quasars (e.g., Reeves & Turner 2000). Indeed, *BeppoSAX* observations of two distant ($z \sim 4$) blazars (Fabian et al. 2001a, 2001b) show the presence of huge absorption, with column density of the order of a few times 10^{23} cm^{-2}.

For three sources (0208−512, 1641+399, and 2251+158) we detect hard X-ray emission up to $\sim$100 keV. For 1641+399 and 2251+158 the hard X-ray component appears to be the smooth extrapolation of the soft–medium X-ray continuum, while in 0208−512 the PDS spectrum is likely contaminated by another source present in the large field of view of the instrument. We note however that 0208−512 is one of the few blazars detected by COMPTEL (Blom et al. 1995) and because of its exceptionally intense flux in the MeV band is considered as a prototype of the so-called MeV blazars. Therefore, we cannot completely exclude the possibility that the spectral component responsible for the MeV flux contributes also in the PDS band, explaining the observed excess.

The modeling of the SEDs shows that FSRQs (except the case of 0521−365; see below) are characterized by jets with Doppler beaming factors larger than 10 and magnetic field of the order of $B \sim 2$–3 G, roughly in equipartition with the emitting electrons. The size of the emitting region is of the order of 10^{16} cm, consistent with the absence of short-timescale variability ($\lesssim$1 day) in this class of blazars. These results confirm, with a larger sample, the conclusions of Paper I.

An interesting issue for blazars is the value of the minimum Lorentz factor of the emitting electrons, $\gamma_{\rm min}$. In Paper I we showed how, from the absence of a spectral break in the soft X-ray continuum, it is possible to infer that the electron energy distribution extends down to $\gamma_{\rm min} \sim 1$. In fact, a break in the EC continuum is expected at the frequency $\nu_{\rm br} \simeq \Gamma^2 \nu_{\rm ext} \gamma_{\rm min} \sim 10^{17}$ Hz (e.g., Sikora et al. 1997), corresponding to an energy of $\sim$1 keV (in the rest frame of the source). We recall that the lack of soft X-ray photons observed in 2251+158 (as for the case of 0836+710 reported in Paper I) could be interpreted as due to such an intrinsic break in the continuum. Observations with larger signal-to-noise ratio (possible with *XMM-Newton* or *Chandra*) will allow us to disentangle the two possible interpretations, intrinsic curved continuum or absorption.

In our fits n_1, the index of the low-energy portion of the electron energy distribution, is smaller than 2. Clearly, such a flat spectrum cannot be produced by the cooling of high-energy electrons (in that case one would expect $n_1 = 2$). On the other hand, this spectrum is even flatter than the standard prediction $n_1 = 2$ for a population of nonthermal electrons produced through Fermi acceleration by a nonrelativistic shock (e.g., Blandford & Ostriker 1978). However, recent calculations (see the review by Kirk & Dendy 2001) show that relativistic shocks, such as those likely present in the jets of blazars, could produce extremely flat ($n_1 < 2$) spectra.

The case of 0521−365 is atypical. Previous observational evidence suggested that the jet forms a relatively large angle with the line of sight. Pian et al. (1996), using independent arguments (in particular the presence of an optical jet; e.g., Scarpa et al. 1999), concluded that $\theta \sim 30°$. Assuming that the bulk Lorentz factor of the emitting plasma is similar to that of the other blazars, $\Gamma_b \sim 10$, this implies that the emission from 0521−365 is weakly boosted ($\delta = 1$–2). The SED reported in Figure 5 has been calculated assuming $\Gamma_b = 10$ and $\theta = 15°$, implying $\delta = 3$. In this situation the X-ray/γ-ray continuum, contrary to the case of the other sources, is dominated by the SSC emission, while the EC spectrum gives only a small contribution in the γ-ray band.

Part of the motivation for this investigation was to study the difference between the EGRET and non-EGRET sources. In the whole FSRQ sample observed with *BeppoSAX* there are nine EGRET sources and three sources not detected by EGRET. The average X-ray spectral indices ($\Gamma_{\rm EGRET} = 1.56 \pm 0.06$ and $\Gamma_{\rm non\text{-}EGRET} = 1.69 \pm 0.07$ for EGRET and no-EGRET sources, respectively) indicate that, within the statistical uncertainty, the X-ray spectral characteristics are similar for both groups. The modeling of the SEDS confirms the strong similarity between the two groups. The lack of the EGRET detection could be attributed to the variability behavior typical of these sources in the γ-ray band (e.g., Mukherjee et al. 1997) rather than to an intrinsic difference in the properties of the jet. New γ-ray missions (*AGILE*, *Gamma-Ray Large Area Telescope*) will help to further investigate these problems.

We thank the *BeppoSAX* SDC for providing us with the cleaned data. This work was partly supported by the ASI grant I-R-105-27-00. This research has made use of the NASA/IPAC Extragalactic Database (NED), which is operated by the Jet Propulsion Laboratory, California Institute of Technology, under contract with the National Aeronautics and Space Administration.

REFERENCES

Bertsch, D. L., et al. 1993, ApJ, 405, L21
Blandford, R. D., & Königl, A. 1979, ApJ, 232, 34
Blandford, R. D., & Ostriker, J. P. 1978, ApJ, 221, L29
Blom, J. J., et al. 1995, A&A, 298, L33
Boella, G., et al. 1997, A&AS, 122, 327
Celotti, A., Padovani, P., & Ghisellini, G. 1997, MNRAS, 286, 415
Dermer, C. D., & Schlickeiser, R. 1993, ApJ, 416, 458
Dermer, C. D., et al. 1995, ApJ, 446, L63
Dondi, L., & Ghisellini, G. 1995, MNRAS, 273, 583
Fabian, A. C., Celotti, A., Iwasawa, K., & Ghisellini, G. 2001a, MNRAS, 324, 628
Fabian, A. C., Celotti, A., Iwasawa, K., McMahon, R. G., Carilli, C. L., Brandt, W. N., Ghisellini, G., & Hook, I. M. 2001b, MNRAS, 323, 373
Falomo, R., Bersanelli, M., Bouchet, P., & Tanzi, E. G. 1993, AJ, 106, 11
Fossati, G., et al. 1998, MNRAS, 299, 433
Garcia, A., Sodré, L., Jr., Jablonski, F. J., & Terlevich, R. J. 1999, MNRAS, 309, 803
———. 1994, MNRAS, 267, 167
Georganopoulos, M., Kirk, J. G., & Mastichiadis, A. 2001, ApJ, 561, 111
Ghisellini, G., et al. 1998, MNRAS, 301, 451
———. 1999, A&A, 348, 63
Glass, I. S. 1981, MNRAS, 194, 795
Gregory, P. C., & Condon, J. J. 1991, ApJS, 75, 1011
Haas, M., Chini, R., Meisenheimer, K., Stickel, M., Lemke, D., Klaas, U., & Kreysa, E. 1998, ApJ, 503, L109
Hartman, R. C., et al. 1999, ApJS, 123, 79
Impey, C. D., & Neugebauer, G. 1988, AJ, 95, 307
Impey, C. D., & Tapia, S. 1988, ApJ, 333, 666
Jones, F. C. 1968, Phys. Rev., 167, 1159

Kaspi, S., Smith, P. S., Netzer, H., Maoz, D., Jannuzi, B. T., & Giveon, U. 2000, ApJ, 533, 631
Kirk, J. G., & Dendy, R. O. 2001, J. Phys. G, 27, 1589
Kotilainen, T. K., Falomo, R., & Scarpa, R. 1998, A&A, 336, 479
Kubo, H., et al. 1998, ApJ, 504, 693
Kühr, H., Pauliny-Toth, I. I. K., Witzel, A., & Schmidt, J. 1981, AJ, 86, 854
Lawson, A. J., & Turner, M. J. L. 1997, MNRAS, 288, 920
Mannheim, K., & Biermann, P. L. 1992, A&A, 253, L21
Maraschi, L., Ghisellini, G., & Celotti, A. 1992, ApJ, 397, L5
Maraschi, L., & Tavecchio, F. 2001, in ASP Conf. Ser. 234, X-Ray Astronomy 2000, ed. R. Giacconi, L. Stella, & S. Serio (San Francisco: ASP), 437
Maraschi, L., et al. 1998, in The Active X-Ray Sky: Results from *BeppoSAX* and *RXTE*, ed. L. Scarsi (Amsterdam: Elsevier), 453
Moshir, M. E. A., et al. 1990, The *IRAS* Faint Source Catalogue, Version 2.0 (Greenbelt: NASA/GSFC)
Mukherjee, R., et al. 1997, ApJ, 490, 116
Neugebauer, G., Sofer, B. T., Matthews, K., Chanan, G. A., & Margon, B. 1982, AJ, 87, 1639
Padovani, P., & Urry, C. M. 1992, ApJ, 387, 449
Patnaik, A. R., Browne, I. W. A., Wilkinson, P. N., & Wrobel, J. M. 1992, MNRAS, 254, 655
Pian, E., Falomo, R., Ghisellini, G., Maraschi, L., Sambruna, R. M., Scarpa, R., & Treves, A. 1996, ApJ, 459, 169
Pian, E., & Treves, A. 1993, ApJ, 416, 130
Pian, E., et al. 1999, ApJ, 521, 112
———. 2002, ApJ, submitted
Reeves, J. N., & Turner, M. J. L. 2000, MNRAS, 316, 234
Sambruna, R. M. 1997, ApJ, 487, 536
Scarpa, R., Urry, C. M., Falomo, R., & Treves, A. 1999, ApJ, 526, 643
Siebert, J., Brinkmann, W., Drinkwater, M. J., Yuan, W., Francis, P. J., Peterson, B. A., & Webster, R. L. 1998, MNRAS, 301, 261
Sikora, M., Begelman, M. C., & Rees, M. J. 1994, ApJ, 421, 153
Sikora, M., Madejski, G., Moderski, R., & Poutanen, J. 1997, ApJ, 484, 108
Smith, P. S., Elston, R., Berriman, G., Allen, R. G., & Balonek, T. J. 1988, ApJ, 326, L39
Stacy, J. G., Vestrand, W. T., Sreekumar, P., Bonnell, J., Kubo, H., & Hartman, R. C. 1996, A&AS, 120, 549
Stevens, J. A., Litchfield, S. J., Robson, E. I., Hughes, D. H., Gear, W. K., Teräsranta, H., Valtaoja, E., & Tornikoski, M. 1994, ApJ, 437, 91
Tavecchio, F., et al. 2000, ApJ, 543, 535 (Paper I)
Thompson, D. J., et al. 1995, ApJS, 101, 259
Tornikoski, M., et al. 1996, A&AS, 116, 157
Urry, C. M., & Padovani, P. 1995, PASP, 107, 803
Villata, M., et al. 1997, A&AS, 121, 119
Wiren, S., Valtaoja, E., Teräsranta, H., & Kotilainen, J. 1992, AJ, 104, 1009
Wright, A., & Otrupcek, R. 1990, PKS Catalog
Wright, A. E., Ables, J. G., & Allen, D. A. 1983, MNRAS, 205, 793
Wright, A. E., Griffith, M. R., Hunt, A. J., Troup, E., Burke, B. F., & Ekers, R. D. 1996, ApJS, 103, 145
Xie, G. Z., Zhang, X., Bai, J. M., & Xie, Z. H. 1998, ApJ, 508, 180